Journal of Building Engineering 4 (2015) 283–294

Contents lists available at ScienceDirect

Journal of Building Engineering

journal homepage: www.elsevier.com/locate/jobe

An experimental evaluation of prediction models for the mechanical behavior of unreinforced, lime-mortar masonry under compression

Adrian Costigan, Sara Pavía *, Oliver Kinnane

Department of Civil, Structural and Environmental Engineering, Trinity College Dublin, Ireland

ARTICLE INFO

Article history:
Received 11 December 2014
Received in revised form
9 September 2015
Accepted 1 October 2015
Available online 9 October 2015

Keywords:
Lime mortar masonry
Brick-masonry compressive strength
Mortar strength
Masonry elastic modulus
Masonry stress–strain

ABSTRACT

This paper contributes to the understanding of lime-mortar masonry strength and deformation (which determine durability and allowable stresses/stiffness in design codes) by measuring the mechanical properties of brick bound with lime and lime-cement mortars. Based on the regression analysis of experimental results, models to estimate lime-mortar masonry compressive strength are proposed (less accurate for hydrated lime (CL90s) masonry due to the disparity between mortar and brick strengths). Also, three relationships between masonry elastic modulus and its compressive strength are proposed for cement-lime, hydraulic lime (NHL3.5 and 5), and hydrated/feebly hydraulic lime masonries respectively.

Disagreement between the experimental results and former mathematical prediction models (proposed primarily for cement masonry) is caused by a lack of provision for the significant deformation of lime masonry and the relative changes in strength and stiffness between mortar and brick over time (at 6 months and 1 year, the NHL 3.5 and 5 mortars are often stronger than the brick). Eurocode 6 provided the best predictions for the compressive strength of lime and cement-lime masonry based on the strength of their components. All models vastly overestimated the strength of CL90s masonry at 28 days however, Eurocode 6 became an accurate predictor after 6 months, when the mortar had acquired most of its final strength and stiffness.

The experimental results agreed with former stress–strain curves. It was evidenced that mortar strongly impacts masonry deformation, and that the masonry stress/strain relationship becomes increasingly non-linear as mortar strength lowers. It was also noted that, the influence of masonry stiffness on its compressive strength becomes smaller as the mortar hydraulicity increases.

1. Introduction

Masonry has historically been a common and successful means of cladding and loadbearing structures. Today, it constitutes a considerable proportion of buildings worldwide that are often of historic and cultural significance. Masonry is a heterogeneous material with a complex, non-linear, anisotropic behavior (when compared to materials such as concrete or steel) which can be attributed to the different material components and the abundant interfaces. For centuries, masonry was bound with lime mortars. However, as most limes build strength slowly mainly by carbonation, they were superseded, first by hydraulic limes, and then by Portland Cement (PC) which develops strength quickly on hydration. However, for over two decades, there has been a renewed focus on the use of hydrated and hydraulic lime-mortars for repairs and new building. This paper intends to contribute to the understanding of the characteristics of lime-mortar masonry. The knowledge of masonry strength and deformation characteristics is important as these determine masonry performance over time and allowable stress and stiffness in design codes for new building.

Mechanical properties and behavior are well documented for cement mortar masonry but there continues to be a paucity of literature on the performance of lime-mortar masonry. Masonry compressive strength and other mechanical properties can be measured experimentally in the laboratory however, the tests are intense in materials and labor. This lead to a search for analytical relations to predict masonry strength based on the properties of masonry components (which can be taken from manufacturers specifications or tested at a lower cost). This paper experimentally measures the compressive strength, modulus of elasticity and stress–strain behavior of fired-clay brick masonry bound with mortars of varying strength and stiffness including hydrated lime

* Correspondence to: Department of Civil Engineering, Museum Building, Trinity College Dublin, Dublin 2, Ireland.
E-mail address: pavias@tcd.ie (S. Pavía).

http://dx.doi.org/10.1016/j.jobe.2015.10.001

Table 1
Summary of models for the estimation of masonry strength

Source reference	Model	
Eurocode 6 [8,22]	$f'_m = 0.5 f_b^{0.7} f_j^{0.3}$	(2)
Bennett et al. [17]	$f'_m = 0.3 f_b$	(3)
Dayaratnam [18]	$f'_m = 0.275 f_b^{0.5} f_j^{0.5}$	(4)
MSJC [19]	$f'_m = (400 + 0.25 f_b)/145$	(5)
Kaushik et al. [10]	$f'_m = 0.63 f_b^{0.49} f_j^{0.32}$	(6)
Gumaste and Venkatarama Reddy [20]	$f'_m = 0.317 f_b^{0.866} f_j^{0.134}$	(7)
Hendry and Malek [21]	$f'_m = 0.317 f_b^{0.531} f_j^{0.208}$	(8)

(CL90s), natural hydraulic lime (NHL) and a cement-lime mortar (M6). Regression analysis was applied to the experimental results and models for the estimation of lime-mortar masonry compressive strength proposed. A general model was derived and alternative models that consider strong hydraulic and weak limes only were also proposed with different fitnesses. In addition, cement masonry models, previously documented in the literature, were reviewed and their appropriateness for the description of lime-mortar masonry assessed by comparing the experimental results from this study with the values calculated using these models. Also, using regression analysis, equations are developed for the estimation of the elastic modulus of lime-mortar masonry; and stress–strain curves are derived for the various types of lime-mortar masonry. Finally, stress–strain estimation models in the literature are compared with the experimental stress–strain relationships determined in this research.

1.1. Behavior of masonry under uniaxial compression

Zucchini and Lourenço [1] developed a homogenization model where they summarize the behavior of brick masonry under compression including simple compression failure theories in former research [2,3] and experimental results by former authors [4–7], who, using experimental data, suggested several analytical relations to estimate masonry strength and deformation which depend on the compressive and tensile strengths of bricks and mortar and other factors. As explained by Zucchini and Lourenço [1], when weak mortars are in place, the non-linear (plastic) deformation of the mortar starts very early on loading, while the brick plastic behavior begins later. The brick is in a tension–compression–tension state, while the mortar is in a tri-axial compression state because of the lateral confinement of the stiffer brick. As a result, the joint suffers some negligible damage in tension but it is the failure of the brick in tension that leads to masonry failure. According to McNary and Abrams [4], under compression, a softer mortar increases the lateral tensile stress applied to the brick decreasing the stiffness of the masonry. These authors also noted that the relation between stress and strain becomes increasingly non-linear as mortar strength lowers.

Zucchini and Lourenço [1], further explain that when the mortar is stiffer but still weaker in compression than the unit, the brick does not fail in tension because the difference in stiffness between the two components is not sufficient for the brick to reach its limit strength and the masonry fails due to the crushing of the brick. Finally, when the mortar is much stiffer and stronger than the unit, the plastic flow starts earlier in the brick due to the higher mortar strength. The much greater mortar stiffness yields a tension–tension–compression state at the joint which damages the mortar in tension, but the masonry failure is driven again by the crushing of the brick.

These authors conclude that, if the brick compressive strength is sufficiently high, the brick fails in tension and masonry strength is sensitive only to the unit tensile strength. However if the brick strength drops, the masonry failure mode changes from unit cracking in tension to unit crushing in compression with a 14% reduction of the masonry strength. Therefore, according to these authors, only the brick compression strength affects masonry strength; the other properties of the components can only change the deformation path of the masonry.

In historic and traditional fabrics bound with lime mortars the mortar is generally considered weaker, less stiff and more deformable than the masonry units. However certain hydraulic limes, over time, can achieve a greater strength and stiffness than certain pressed, solid or frogged, fired-clay bricks.

1.2. Analytical models for the behavior of masonry under uniaxial compression

As aforementioned, the mechanical behavior and strength of masonry (f'_m) can be measured experimentally however, analytical relations have been proposed to predict masonry strength based on the properties of the masonry components. The majority of models have been developed for strong, cement-based mortars, with few including lime mortars. Eurocode 6 EN1996-1-1 [8] presents a simple analytical model that relates the compressive strength of masonry with the compressive strength of mortar (f_j) and masonry unit (f_b) [8]. Eq. (1) describes the relationship between these parameters as

$$f'_m = K f_b^{\alpha} f_j^{\beta} \tag{1}$$

where, (K, α and β) are constants and the compressive strength of the brick is normalized as described in EN 711-1 [9]. Eurocode 6 is primarily designed for cement mortar masonry with values of K, α and β appropriate for cement mortar bound masonry (Table 1). This study investigates its appropriateness for lime-bound masonry.

As reviewed by other authors studying cement and cement-lime mortars [10,11], further analytical models for the prediction of compressive strength and deformation characteristics of masonry have been proposed by previous researchers [6,12–16]. Usually, these models are not presented as simple analytical relationships. However, based on the regression analysis of experimental data, Bennett et al. [17], using cement mortars, proposed a simple linear relationship between the masonry and brick strength; with the compressive strength of masonry estimated as 0.3 times the brick compressive strength. However, masonry compressive strength (f'_m) can be overestimated since the mortar strength is not taken into account.

When both the mortar and unit strengths are taken into account (as in Eq. (1)), as the brick is usually stronger and stiffer than the mortar, a greater proportion of the masonry compressive strength originates from the brick. Therefore, α would be expected to be a higher value than β. Eurocode 6 [8] defines the values of α and β as 0.7 and 0.3, respectively, and provides a range for K from 0.4 to 0.6. The K value depends on brick type and the brick-mortar joint characteristics. In contrast, equal weights were proposed for α and β by Dayaratnam [18] with a K value of 0.275. Based on a series of experiments and subsequent regression analysis of results, Kaushik et al. [10] proposed values of 0.63, 0.49 and 0.32 for K, α and β. These authors investigated experimental results by former authors and compared them to predicted compressive strength estimates based on Eq. (1) and other equations by Eurocode 6 and [17–19] (see Table 1). They concluded that their equation (Eq. (6)) generally gave a better prediction than the others for masonry prisms made with low and average strength bricks. They also noted that, for brick with a compressive strength greater than 25 N/mm^2, the linear relationship proposed by Bennett et al. [17] (Table 1) provided the best estimate of masonry compressive strength (when the brick is strong and stiff enough the mortar does not impact the strength of the masonry). Gumaste et al. [20], testing bricks with cement and cement-lime mortars (some including soil), proposed values of 0.317, 0.866 and 0.134 for K, α and β and compared their model to that proposed by Hendry and Malek [21] (0.317, 0.531 and 0.208 for K, α and β) found for cement-lime mortars. In this paper, these models are assessed for lime-mortar masonry.

1.3. Analytical models to determine stress–strain relationships in compression

Several authors have investigated the stress–strain relationships developed on uniaxial compression of masonry prisms and wallettes bound with PC based mortars [10,13,15,16]. Eurocode 6 [8] acknowledges that the stress–strain relationship of masonry in compression is non-linear. The code permits the stress–strain curve to be taken as linear (up to $0.33f'_m$) or as a parabolic rising curve (up to a strain of 0.002) and as a horizontal plateau up to 0.0035 of strain. Other authors describe the parabolic rising portion as part of a 'modified' Kent-Park model [10,13,15,16] consisting of a parabolic rising curve, a linear falling branch and a horizontal plateau. Kaushik et al. [10] also considered the ascending part of the masonry stress–strain curve as a parabolic curve (which provided a good fit to experimental data) and proposed Eq. (9) in terms of stress and strain ratios;

$$\frac{f_m}{f'_m} = 2\frac{\varepsilon_m}{\varepsilon'_m} - \left(\frac{\varepsilon_m}{\varepsilon'_m}\right)^2 \tag{9}$$

where, f_m and ε_m are the compressive stress and strain of masonry and ε'_m the peak strain corresponding to f'_m.

To predict the stress–strain relationship, the maximum deformation, or peak strain (ε'_m), under the applied compressive load is an essential parameter. Based on regression analysis of experimental results, Kaushik et al. [10] proposed Eq. (10) to estimate peak strain, where K is set to 0.27 and α to 0.25;

$$\varepsilon'_m = \frac{K}{f_j^{\alpha}}\left(\frac{f'_m}{E_m}\right) \tag{10}$$

The estimation of ε'_m becomes ever more critical when dealing with a deformable material such as lime mortar therefore, this model, which was developed for PC mortar masonry, is evaluated here for lime-mortar masonry.

Structural performance is generally characterized at a variety of limit states. For the stress–strain characterization of confined masonry four performance limit states were shown to correspond to 75% and 90% of prism compressive strength on the rising part of the stress–strain curve and 50% and 20% of prism compressive strength on the falling branch [16]. Based on these limit states and their own experimental results, Kaushik et al. [10] determined 6 control points at 33% (linear portion beyond which cracking occurs), 75% (evidence of vertical splitting in bricks), 90% (excessive splitting) and 100% of the peak compressive strength (f'_m).

The elastic modulus (E_m) is linearly related to the compressive strength of masonry (f'_m) as described by Eq. (11) from Eurocode 6 and adopted by other authors [8,10,15,23–25];

$$E_m = k f'_m \tag{11}$$

Masonry stiffness varies considerably with its compressive strength as evidenced by a wide range of values for k in the literature. Kaushik et al. [10] found by linear regression that the elastic modulus of masonry bound with mortars of variable strength reached values of 250–1100 times the compressive strength. Most authors propose values of 700–750 [15,24] and 1000 for k [8] when studying cement bound masonry. Lime mortar masonry shows a greater deformability than cement bound masonry on loading, therefore stress–strain characteristics, elastic modulus and peak strain are of interest. In this paper, models of lime-mortar masonry deformability with varied accuracy are generated based on the regression analysis of the experimental stress–strain data.

2. Materials and methods

2.1. Materials

Mortars were made with hydrated lime (CL90s) and three NHLs

of hydraulic strengths 2, 3.5 and 5 N/mm^2 complying with EN 459-1 [26]. The reference cement mortar, M6 (Cem II/A-L), is characterized by a minimum compressive strength of 6 N/mm^2 at 28 days. A siliceous aggregate of particle size distribution ranging within standard limits was used. Based on previous research [27,28], initial flows of 165 and 170 ± 3 mm were specified for all mortars to ensure adequate workability. The lime mortars were mixed at a binder: aggregate ratio of 1:3 by weight. Specimens sized 40x40x160 mm^3 were used and the reported values are the arithmetic mean of 4–6 specimens. The initial flow was measured in accordance with EN 459-2 [29] and the water content reported as the ratio of water to total mortar by mass. M6 was mixed in a 1:1/2:4 ratio by volume as specified by EN 196-1 (2005) [29]. Mixing, curing and storage were in accordance with EN 196-1 [30] and EN 459-2 [29].

Masonry wallettes were constructed with machine-pressed, frogged, fired-clay brick according to EN 1052-1 [31]. They were cured and stored in the same conditions as the corresponding mortar. The bricks are characterised by relatively low strength and stiffness, and a high suction (Table 2 - mean of 6 specimens). The mortar strength was measured according to EN196-1 [30] and EN459-2 [29]. The modulus of elasticity (E_c) was found from the linear portion of the stress–strain curve obtained in the compressive strength test. The initial rate of absorption (IRA) measures the initial moisture transfer between brick and mortar. This is essential to develop a proper bond which in turn determines the tensile strength of masonry. The initial rate of absorption (IRA) measures the initial moisture transfer between brick and mortar. This, together with the mortar water retention (ability of mortar to resist water loss), are essential to develop a proper bond which in turn determines the tensile strength of masonry. The initial rate of absorption (IRA) is a property of the brick. It is a measure of how much moisture it absorbs in contact with water in the first minute. In this paper, this is a constant as the same brick was used in all tests.

All the lime mortars used in this research have great water retention characteristics. Values ranging between 84% and 99% have been consistently determined [27,28]. The importance of the IRA and water retention of the mortar on the strength of the bond was investigated in detail by Hanley and Pavía [27] and Pavía and Hanley [28]. The transfer of moisture is also determined by the mass structure and pore system characteristics therefore, the density and open porosity were also measured.

2.2. Mortar properties

Mortar compressive strength tests were conducted according to EN196-1 [30] with modifications from EN 459-2 [30]. The applied load was increased smoothly at a rate of 400 ± 40 N/s until failure occurred, as per EN 459-2. The test machine used is equipped with an internal load cell and a displacement-meter recording the force applied, displacement and strain over time. The compressive strength was calculated using Eq. (12) below where, R_c is the compressive strength, in N/mm^2; F_c is the maximum load at fracture in Newtons; and 6400 is the area of the prism face in mm^2 (160 × 40). The flexural strength of the mortar was determined using the three point flexural test in accordance with EN 196-1 [30] Eq. (13) where, R_f is the flexural strength (N/mm^2); F_f is the load applied to the middle of the prism at fracture (in Newtons); b is the side of the square section of the prism, in mm; and l is the distance between the supports (in mm).

Table 2
Properties of fired-clay brick used in this study; R_c compressive strength; fb normalized compressive strength; { } coefficient of variation.

Property/standard	Values	
Unit size (mm)	215 × 102.5 × 65	
Compressive strength (N/mm^2)/EN 772-1 [32]	R_c	f_b
	15.0 {5.9}	12.75
Tensile strength (N/mm^2) EN 12372 [33]	2.63 {4.33}	
Modulus of elasticity (E_c) (N/mm^2)	1240 {7.5}	
Density (Kg/m^3)/EN 1936 [34]	1920	
Open porosity (%)/EN 1936 [34]	15	
IRA (brick)/EN 772-11 [35]	1 kg/m^2/min	

$$R_c = \frac{F_c}{6400} \tag{12}$$

$$R_f = \frac{1.5 \times F_f \times l}{b^3} \tag{13}$$

The mortar elastic modulus was determined as the slope of the linear portion of the stress–strain curve between approximately 30–50% of the ultimate stress. Vertical displacement was recorded using the testing machine's internal meter. To avoid errors, the displacement meter was zeroed at the time at which the internal load cell registered a reading. The strain was calculated by dividing the distance traveled by the original height of the specimen (40 mm). The following equations (Eqs. (14)–(16)) were used to calculate the modulus of elasticity in compression:

$$\sigma = \frac{F_x}{A_i} \tag{14}$$

$$\epsilon = \frac{\Delta h}{h_0} \tag{15}$$

$$E_c = \frac{\sigma_{50} - \sigma_{30}}{\varepsilon_{50} - \varepsilon_{30}} \tag{16}$$

where, E_c is the modulus of elasticity; σ and ε are the compressive stress and strain at any point on the stress–strain curve; Fx is the applied force; A_i is the loaded cross-sectional area; Δh is the change in height of the specimen, due to the applied force; h_0 is the original height of the specimen.

2.3. Masonry compressive strength and stress strain characterization

The masonry compressive strength was tested according to EN 1052-1 [31] at 28 and 56 days, 6 months and 1 year intervals. During the tests, force–strain curves were recorded with the strain values provided by linear variable displacement transducers continuously monitoring the change in length on application of the load. Eqs. (17) and (18) were used to determine the compressive (f_i) and characteristic (f_k) compressive strength. Where: $F_{i,max}$ is the maximum load (N) and A_i is the loaded cross-section (mm^2).

$$f_i = \frac{F_{i,max}}{A_i} \left(\mathrm{N/mm^2}\right) \tag{17}$$

$$f_k = \frac{f}{1.2} \text{ or } f_k = f_{i,\,min} \text{ whichever is smaller } \left(\mathrm{N/mm^2}\right) \tag{18}$$

As discussed below, the stress–strain curves of brick masonry displayed a significant initial concave section due to early large deformation of lime-mortar and settling of the testing assembly (see Fig. 1 (left)). This portion was corrected, using the procedure documented by Vermeltfoort [24] to enable comparison with cement-mortar masonry results. The stress–strain curves were first normalized by letting $\sigma_r = \sigma/\sigma_{max}$ and $\varepsilon_r = \varepsilon/\varepsilon_{r,90,}$ where σ_{max} is the

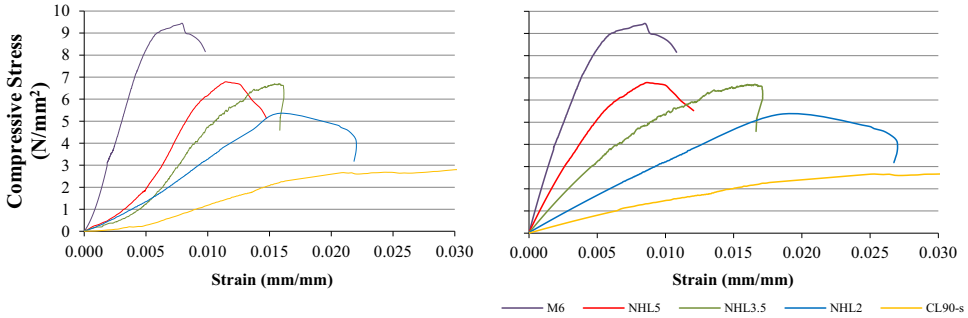

Fig. 1. Masonry stress–strain curves (left) and corrected curves (right) after 2 months of curing.

ultimate stress and $\varepsilon_{r,90}$ is the strain at $0.9\sigma_{max}$. Omitting the results in the concave portion and using a best fit quadratic procedure, a curve is described with the general form of Eq. (19) between approximate normalized stresses of 0.3 and 0.9.

$$\sigma_r = A\left(\epsilon_r\right) + B(\epsilon)_r^2 \tag{19}$$

The origin becomes the point where the parabolic curve crosses the strain axis (see Fig. 1(right)). The concave portion of the stress–strain curve is then replaced by the lower portion of the parabolic curve and the corrected curve is rescaled in the ratio of $\varepsilon_{r,90}$ to $\varepsilon_{r,max}$.

The standard for cement and cement-lime masonry EN 1052-1 [31] describes the modulus of elasticity (E_m) as the secant of the stress–strain curve at 33% of the ultimate stress, and other authors have used other methods [40,10]. However, due to the non-linear behavior of lime mortar masonry, the 33% point is often not in the linear portion of the stress–strain curve. Therefore, in this study E_m is calculated as the slope of the linear portion of the stress–strain curve (obtained during the masonry compressive strength test) lying between 30% and 50%.

2.4. Regression analysis of experimental data

As aforementioned, Eurocode 6 relates masonry compressive strength to brick and mortar compressive strength as described in Equation 1 with constants K, α and β. Using regression analysis based on the least-squares fit method [10], these parameters are estimated for all lime-mortars at discrete times during curing. By regression of experimental data, Eq. (1) is estimated for the range of lime bound masonry subject to study at different curing ages. This equation is rearranged to $f'_m - Kf_b^{\alpha} f_j^{\beta} = 0$ and "least squares" regression analysis carried out whereby, K, α and β are systematically varied in order to minimize the sum of square errors (SSE);

$$SSE = \sum (f_i - f_{Ri})^2 \tag{20}$$

where, fi is the ith experimental prism strength, fRi is the ith regression estimate of masonry strength. The fitness of the models was evaluated using the coefficient of determination (R^2) and standard error of estimate (σ) given by Eqs. (21) and (22) respectively;

$$R^2 = 1 - \sqrt{\frac{\sum (f_i - f_{Ri})^2}{\sum (f_i - f_{mean})^2}} \tag{21}$$

$$\sigma = \sqrt{\frac{\sum (\boldsymbol{f_i} - \boldsymbol{f_{Ri}})^2}{\boldsymbol{n} - 3}} \tag{22}$$

where, f_{mean} is the arithmetic average of experimentally obtained masonry strengths and n represents the number of data points investigated.

In order to carry out the regression analysis of experimental masonry peak strain (ε'_m) data, Equation 10 is rearranged to $\varepsilon'_m - \frac{K}{f_j^{\alpha}}\left(\frac{f'_m}{E_m}\right) = 0$ and "least squares" regression analysis carried out whereby, K, and α are systematically varied, following the same procedure outlined above (Eqs. (20)–(22)), in order to minimize the sum of square errors (SSE). Since two estimators K and α are desired, $n-2$ degrees of freedom are used in the calculation of σ, in order to achieve an unbiased estimate.

3. Experimental results

3.1. Mechanical properties of mortars and masonry

The properties of the brick (f_b), the different mortars (f_j) and the brick masonry walletes (f'_m)) are included in Tables 2–4 respectively.

As can be seen from Tables 2 and 3, initially, the brick ($f_b = 12.7$ N/mm^2; $E_c = 1240$ N/mm^2) is stronger and stiffer than all the mortars however, at 6 months and 1 year, hydraulic lime mortars NHL 3.5 and 5 show similar strength to the brick although much lower stiffness. After the initial month, the PC-lime mortar (M6) is stronger and stiffer than the brick.

The M6 and NHL 5 mortars are stronger in compression than their masonries at all times (except for the NHL5 mortar at 28 days). In contrast, lower strength mortars NHL 2 and CL90s are weaker than their masonries at all times. The cement-lime mortar, M6, has nearly twice the masonry strength at 28 days however, over time, the differences become greater and, at 6 months, the M6 mortar is nearly 3 times stronger than its masonry. In contrast,

Table 3
Mechanical properties of mortars mixed at 165 mm initial flow. { } coefficient of variation.

Mortar CEM:lime:sand	Mortar compressive strength f_j (N/mm^2)				Mortar flexural strength R_f (N/mm^2)				Mortar elastic modulus E_c (N/mm^2)			
	28 days	56 days	6 months	1 year	28 days	56 days	6 months	1 year	28 days	56 days	6 months	1 year
NHL5 0:1:3	3.9{2}	6.3{3}	11.9{4}	13.3{2}	1.2{10}	1.8{6}	2.5{18}	2.9{8}	278{10}	501{15 }	661{23 }	683{17 }
NHL3.5 0:1:3	3.9{4}	5.2{4}	8.9{5 }	10{5}	0.6{12}	0.7{9}	1{36}	1.3{8}	184{21}	278{11}	387{16}	401{23}
NHL2 0:1:3	1.9{8}	2.3{3}	2.6{13}	2.7{6}	0.3{11}	0.4{7}	0.5{5}	0.6{3}	130{6}	187{6}	165{7}	197{13}
CL90 0:1:3	0.6{21}	0.9{15}	1.4{21}	1.4{20}	0.2{10}	0.3{1}	0.4{12}	0.5{3}	70 {19}	72{28}	107{9}	119{18}
M6 1:0.5:4	11.2{13}	18 { 4}	22.2{16}	–	3{4}	4 {9}	4.8{9}	5.3{5}	927{5}	1380{8}	1587{15}	1744{14}

Table 4
Mechanical properties of brick masonry measured in the laboratory (mortars mixed at 165 mm initial flow). { } coefficient of variation. [a] masonry strength with mortar mixed to 165mm flow.

Masonry mortar	CEM: lime: sand	Masonry compressive strength f'_m (N/mm^2)				Masonry elastic modulus E_m (N/mm^2)			
		28 days	56 days	6 months	1 year	28 days	56 days	6 months	1 year
NHL5	0:1:3	5.4{7} 4.57[a]	6.3{14} 6.79[a]	8.0{6} 6.68[a]	8.5{8}	607{12}	993{11}	1409{7}	1528{3}
NHL3.5	0:1:3	5.0{3} 4.23[a]	5.9{2} 6.7[a]	7.7{12} 6.43[a]	8.9{2}	385{24}	568{11}	842{31}	970{10}
NHL2	0:1:3	3.9{3} 3.25[a]	4.5{13} 5.36[a]	4.8{8} 4.00[a]	4.8{8}	302{9}	361{17}	504{15}	542{24}
CL90s	0:1:3	0.9{15} 0.74[a]	1.5{21} 1.52[a]	3.9{11} 3.28[a]	4.3{6}	196{18}	244{11}	296{31}	317{9}
M6	1:0.5:4	6.9{8} 5.75[a]	7.7{4} 9.46[a]	9.7{12} 8.12[a]	_	1435{9}	1634{5}	2270{15}	–

[a] Masonry strength with mortar mixed to 165 mm flow.

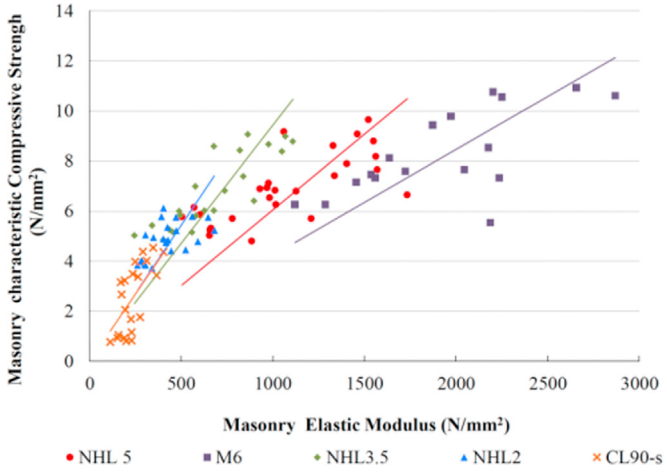

Fig. 2. Relationship between the compressive strength and modulus of elasticity of brick masonry bound with different mortars including hydrated lime (CL90s), hydraulic limes (NHL) and PC-lime mortar (M6) based on experimental results.

Table 5
Correlation between masonry elastic modulus and its characteristic compressive strength based on experimental data.

Masonry mortar CEM:lime:sand	Relationship between masonry elastic modulus (E_m) and its characteristic compressive strength (f'_m)	R^2
NHL5 0:1:3	$E_m = 158 f'_m$	0.51
NHL3.5 0:1:3	$E_m = 102\ f'_m$	0.68
NHL2 0:1:3	$E_m = 88 f'_m$	0.46
CL90 0:1:3	$E_m = 82 f'_m$	0.48
M6 1:0.5:4	$E_m = 231 f'_m$	0.63

the hydrated lime (CL90s) masonry shows greater strength increase over time than its mortar: between 2 months and 1 year, the CL90s masonry triplicates its strength while the CL90s mortar does not even double it. With respect to NHL3.5, the ultimate strength of the NHL3.5 mortar (at 6 months and 1 year) is approximately 24% lower than that of the NHL5 mortar however, their masonries show very similar strength, as shown in Fig. 1.

Costigan and Pavía [36–38] evidenced that the hydraulic grade of the binder (and thus the mortar compressive strength) significantly influences masonry compressive strength, but the impact becomes progressively smaller as the masonry strength moves towards its maximum (which is closely related to the brick's lateral tensile and compressive strength). The compressive strength of the brick masonry was found to tend towards a maximum of approximately 9 N/mm^2 (circa 75% of the normalized compressive strength of the brick). The authors found that the influence of mortar compressive strength on masonry compressive strength was non-linear (with a strong R^2 of 0.795) and related to the ratio of brick strength to mortar strength, i.e. the greater the strength of the mortar with respect to the brick, the smaller the influence of mortar strength variations on the masonry strength. They evidenced that mortars of higher hydraulic strength (M6, NHL 5 and 3.5) were stronger than their corresponding masonry. At 6 months, M6 mortar was over twice stronger than its masonry; NHL 5 mortar was also stronger (11.89 N/mm^2) than its masonry (8.01 N/mm^2), and NHL 3.5 mortar followed a similar trend (8.95 vs. 7.71 N/mm^2). In contrast, lower strength mortars, NHL 2 and CL90-s, were weaker than their masonries (2.62 N/mm^2 and 1.39 N/mm^2 respectively while their corresponding masonry strengths are greater, at 4.8 N/mm^2 and 3.94 N/mm^2 respectively). Costigan and Pavía [36–38] indicate that in the case of higher strength hydraulic limes and cement-lime mortars, substantial increases in mortar compressive strength during curing, do not lead to significant increases in masonry compressive strength over the same timeframe. For example, between 28 and 56 days, the

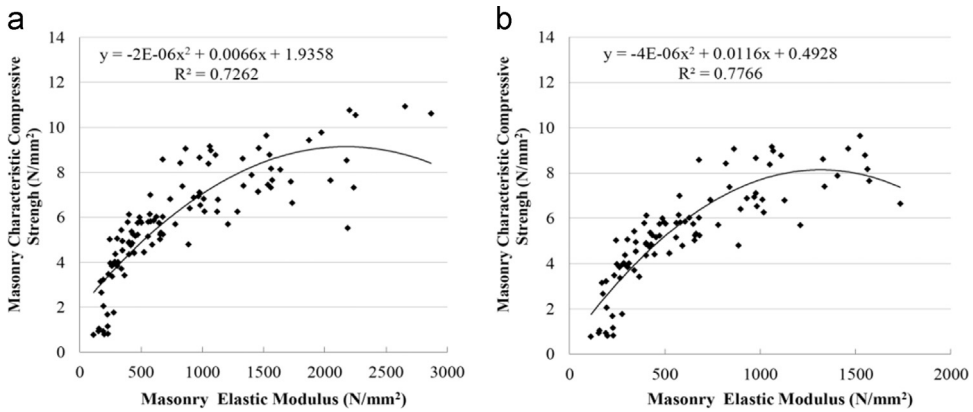

Fig. 3. Relationship between compressive strength and modulus of elasticity for masonry with (a) all mortars (including PC-lime mortar) and (b) lime-mortars only.

Table 6
Equations proposed for the estimation of lime masonry and PC-lime masonry compressive strength based on the regression analysis of experimental data. Coefficient of determination (R^2) and standard error of estimate (σ)

Morta	Regression model for the estimation of masonry compressive strength		R^2	σ (N/mm^2)
All limes (NHL & CL90s)	$f'_m = 0.56 f_b^{0.53} f_j^{0.5}$	(23)	0.78	0.87
NHL only	$f'_m = 0.69 f_b^{0.55} f_j^{0.37}$	(24)	0.96	0.44
CL90s only	$f'_m = 0.55 f_b^{0.5} f_j^{0.5}$	(25)	0.75	1.12
M6 only	$f'_m = 0.46 f_b^{0.5} f_j^{0.5}$	(26)	0.99	1.02

Table 7
Estimation of compressive strengths of brick masonry bound with lime and PC-lime mortars using the regression models in Table 6. Values in {} represent the percentage error between experimental and model estimated results.

Masonry compressive strength f'_m calculated using regression models (Table 6) and % error with experimental results (N/mm^2)						
Masonry	Age	f'_m exp.	All limes model (Eq. (23))	NHL only model (Eq. (24))	CL90 only model (Eq. (25))	M6 only model (Eq. (26))
NHL5	28 days	4.57	4.25 {−7}	4.46 {1}	–	–
	6 months	6.68	7.07 {6}	7.14 {7}	–	–
NHL3.5	28 days	4.23	4.24 {0}	4.45 {5}	–	–
	6 months	6.43	6.36 {−1}	6.28 {−2}	–	–
NHL2	28 days	3.25	2.95 {−9}	3.58 {10}	–	–
	6 months	4.00	4.04 {1}	3.62 {−9}	–	–
CL90	28 days	0.74	1.70 {130}	–	1.55 {109}	–
	6 months	3.28	3.20 {−3}	–	1.55 {−53}	–
M6	28 days	5.75	–	–	–	5.50 {−4}
	6 months	8.12	–	–	–	7.74 {−5}

compressive strength of NHL 3.5 and NHL 5 mortar increased by 37% and 64% respectively while the corresponding masonry only increased by 15% and 16%. The same relationship was maintained between 56 days and 6 months. In contrast, non-hydraulic (CL90s) and feebly hydraulic lime (NHL 2) which are much weaker and less stiff than the brick, show the opposite trend: small increases in mortar compressive strength are linked to relatively large gains in masonry compressive strength.

Francis et al. [39] studied the effect of joint thickness on compressive strength of brickwork. They concluded that the thinner the joints the stronger the brickwork; and they noted a greater strength loss with increase in joint thickness for perforated bricks than for solid bricks which they attributed to their lower lateral tensile strength. In this research all bricks were solid (frogged), and the width of the joint was kept approximately regular at circa 12 mm.

3.2. Stress–strain characteristics of masonry

The stress–strain characteristics of the lime-mortar masonries, investigated at 56 days, are shown in Fig. 1. Given the large initial deformation of lime-mortar, the early concave section of the curve is significantly pronounced, particularly for weak mortars. In the low strength masonries bound with NHL 2 and CL90s mortars, large deformations can be seen during early compression due to early plastic mortar deformation, closing of material gaps and settling of testing assembly. In the NHL masonries, an initial plastic deformation is followed by an upward, more or less linear segment between 30% and 60% of the ultimate stress. Generally, above 60% ultimate stress, the relationship is no longer linear, the peak stress is reached, and the material fails. The M6 masonry behaves in a different manner: initially, it absorbs high stress with little deformation and later it suddenly fails with very little plastic deformation. The results evidenced that the properties of the mortar have a strong impact on the deformation of masonry. As noted by former authors [14] the relationship between stress and strain becomes increasingly non-linear as mortar strength decreases.

3.3. Relationship between masonry elastic modulus and compressive strength

The laboratory results in Table 4 are plotted to find the relationship between the elastic modulus and compressive strength of brick masonry bound with the range of mortars investigated (Fig. 2 and Table 5). As aforementioned, the elastic modulus of the brick is 1240 N/mm^2 (Table 2) and the elastic moduli of the mortars vary between 70–1700 N/mm^2 (Table 3).

According to the experimental results, the masonry elastic modulus (E_m) reaches values between 82 and 231 times its characteristic compressive strength (Table 5) and, as the hydraulic

Table 8
Equations proposed to estimate masonry elastic modulus based on the regression of experimental data. E_m – masonry elastic modulus; f'_m - characteristic masonry compressive strength; coefficient of determination (R^2).

Mortar Masonry	Relationship found using experimental data (N/mm^2)	R^2	Regresion models proposed for the estimation of masonry elastic modulus (N/mm^2)	
PC-lime M6	$E_m=231f'_m$	0.63	$E_m=230f'_m$	(27)
Hydraulic lime NHL5	$E_m=158f'_m$	0.51	$E_m=130f'_m$	(28)
NHL3.5	$E_m=102f'_m$	0.68		
Feebly hydraulic NHL2	$E_m=88f'_m$	0.46	$E_m=85f'_m$	(29)
hydrated lime CL90s	$E_m=82f'_m$	0.48		

grade of the mortar increases, the slope of the relationship between f'_m and E_m decreases. Hence the influence of masonry stiffness on the compressive strength of brick masonry becomes smaller as mortar hydraulicity rises. The relationship between masonry elastic modulus and compressive strength has often been assumed as linear [8,10,15,23–25], with only some authors presenting a nonlinear relationship [41]. A nonlinear relationship is documented in this study for all mortars (Fig. 3a) and lime mortars only (Fig. 3b). Therefore, according to the results, the best function that fits the full data set is non-linear (Fig. 3), whereas for each limited data set (each mortar type) the best fit is linear (Fig. 2 and Tables 5 and 8).

4. Models for the estimation of masonry compressive strength, elastic modulus and peak strain obtained from regression analysis of the experimental data

Models for the estimation of masonry compressive strength obtained from regression analysis of the experimental data in this research are included in Table 6 and Fig. 4 below. As aforementioned, Eq. (1) relates the compressive strengths of brick (f_b), mortar (f_j) and masonry (f'_m)) as follows: $f'_m=Kf_b^{\alpha}f_j^{\beta}$. Regression analysis of the experimental data in this research resulted in values for K, α and β of 0.56, 0.53 and 0.5 respectively resulting in Eq. (23) (Table 6) which is proposed to represent lime mortar masonry after 28 days curing. Due to the wide disparity between mortar and brick compressive strengths, particularly for the lower strength lime (CL90s), further regression analysis of the experimental data was undertaken, treating the NHL and CL90s mortars separately (Eqs. (24) and (25) respectively). Similarly, a model specific to cement-lime M6 mortar is presented (Eq. (26)).

As can be seen from Table 7, the accuracy of the predictive models proposed vary. Eq. (23) provided good estimates of compressive strength for NHL-bound masonry. In contrast, poor predictions were found for the compressive strength of hydrated lime (CL90s) masonry which was overestimated by up to 130%, this is due to the large difference between mortar and brick compressive strengths. Again as can be seen from Table 7, removing the CL90s results from the regression (Eq. (24)) improves the strength estimate of NHL brick-masonry to within 10% of experimental values ($R^2=0.96$, $\sigma=0.44$). The wide variation in the CL90s masonry results are most likely primarily related to the ratio of unit strength to mortar strength, and probably due to the great difference in stiffness between the mortar and the masonry unit. Hydrated lime (CL90s) masonry is considered independently by Eq. (25) however,

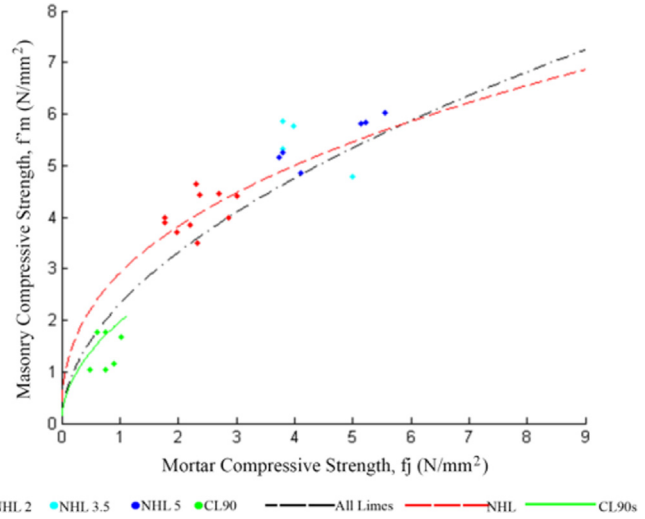

Fig. 4. Plots of Equations 23-26 proposed for masonry compressive strength for All limes, NHL only, CL90s and PC-lime M6 as given in Table 6.

values of $R^2=0.75$ and $\sigma=1.12$ N/mm^2 indicate wide variation within the results. The estimates for CL90s become more accurate with time as the difference between the compressive strength of the mortar and brick becomes smaller. Eq. (26) provides good estimates for the compressive strength of PC-lime (M6) masonry at 28 days. However, it slightly loses accuracy as the mortar increases strength becoming stronger than the brick.

With respect to the masonry elastic modulus (E_m), as aforementioned, it is linearly related to compressive strength (f'_m)) as described by Eurocode 6: $E_m=kf'_m$. The k values found using the experimental data in this research (Table 8) are lower than those reported by previous authors for cement bound masonry (700–1000, [8,15,24]). This is due to the low stiffness and large deformability of lime mortar masonry. Although these models offer good indicative behavior (see deviation from experimental data in Table 9), the coefficients of determination (R^2) are low, particularly for the lower hydraulic strength mortars, due to the lower stiffness of these mortars. Based on the regression analysis of the experimental data, three relationships are proposed for the estimation of the elastic modulus of PC-lime, hydraulic lime and feebly hydraulic/hydrated lime masonry respectively (Table 8 and Fig. 5).

As aforementioned, being able to estimate the amount of deformation masonry will undergo prior to failure is important when dealing with a deformable material such as lime mortar. Kaushik *et*

Table 9
Experimental results and model estimations of the elastic modulus of masonry bound with lime and PC-lime mortars. Based on 56 day results. Values in {} represent the percentage error between experimental and model estimated results. f_j – mortar compressive strength at 170 mm flow.

Experimental and model estimates of masonry elastic modulus E_m and % error with experimental results					
Masonry	Measured properties (56 days)			E_m Calculated using models in Table 8 (Eqs. (27)–(29))	
	f'_m	E_m	f_j	E_m calculated using lab measured f'_m (N/mm^2)	E_m calculated using regression f'_m values (Eqs. (23)–(26)) (N/mm^2)
NHL5	6.79	1127.9	7.02	882.7 {−22}	732 {−35}
NHL3.5	6.7	738.5	6.11	871 {18}	688 {−7}
NHL2	5.36	425.0	2.35	455.6 {7}	387 {−7}
CL90	2.66	175.8	1.52	226.1 {29}	132 {−25}
M6	9.43	1874.0	19.23	2168.9 {16}	1656 {−12}

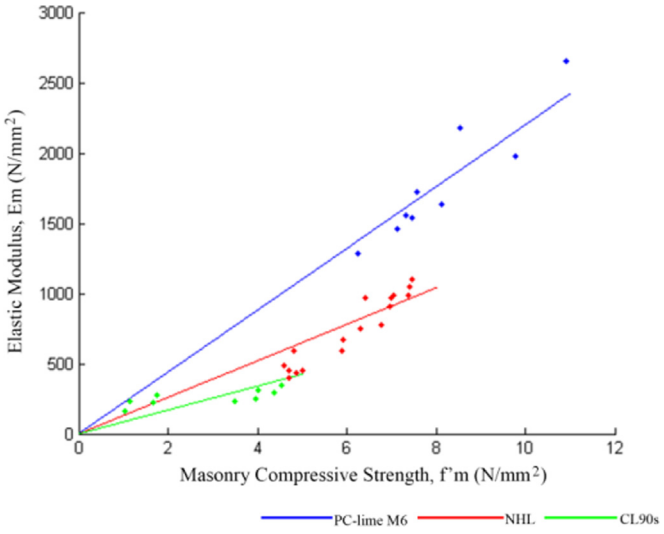

Fig. 5. Plots of Eqs. (27)–(29) proposed for the estimation of masonry elastic modulus for NHL only, CL90s and PC-lime M6 as given in Table 8.

al.[10] proposed Equation 10 to estimate the masonry peak strain, where K is set to 0.27 and α to 0.25: $\varepsilon'_m = \frac{K}{f_j^{\alpha}}\left(\frac{f'_m}{E_m}\right)$. In general, it was found that Eq. (10) significantly underestimates the peak strain value of lime and cement-lime masonry (Table 10). Therefore, regression analysis was used to establish alternative values for K and α which were found at 0.34 and 0.01 respectively (Eq. (30)). These provided a more accurate estimate of masonry strain with R^2 and σ at 0.93 and 0.0003 respectively indicating good correlation. However, as it can be seen from Table 10, the percentage error with the masonry peak strain experimentally measured is still high; and peak strain is underestimated between 73% and 82% (increasing to 75–84% when regression values of f'_m and E_m are used) therefore, the equation deducted by regression does not provide an accurate prediction of masonry peak strain.

$$\varepsilon'_m = \frac{0.34}{f_j^{0.01}}\left(\frac{f'_m}{E_m}\right) \tag{30}$$

5. Comparison of experimental results with prediction models developed for cement-mortar masonry

As reviewed, various authors have developed models to predict the compressive strength of cement and cement-lime masonry based on the strength of the components (Table 1). The accuracy of these models for the characterization of lime-mortar masonry is studied below (Table 11). Masonry compressive strengths f'_m are calculated using unit and mortar compressive strength values documented in Tables 2 and 3 respectively.

The models of the various authors described by the equations in Table 1 are shown graphically in Fig. 6 with the f'_m values from Table 11 marked. Only those models that take account of mortar compressive strength f_j are included.

As can be seen form Table 11, Eurocode 6 provides the best predictions for the estimation of the compressive strength of lime and cement-lime masonry. Eurocode 6 vastly overestimates the strength of the weak, hydrated lime mortar (CL90s) masonry at 28 days but becomes an accurate predictor at 6 months, when the mortar has acquired most of its final strength and stiffness. All the models vastly overestimate the characteristic 28 day compressive strength of hydrated lime (CL90s) bound masonry however their predictions become more accurate at 6 months (0–17% error). Except for Eurocode 6, the models significantly underestimate the compressive strength of the hydraulic NHL3.5/5 lime and lime-cement (M6) masonry at all times (an exception is the NHL3.5 masonry at 28 days, whose strength is underestimated, by all models, with a 10% error (Table 11). In most cases, all the models,

Table 10
Experimental results and model estimations masonry peak strain. Values in {} represent the percentage error between experimental and model estimated results.

Experimental and model estimates of masonry peak strain ε_m and % error with experimental results					
Masonry type	ε_m Measured in the laboratory	ε_m Estimated using Equation 10 by Kaushik et al. [10]		ε_m Estimated using Eq. (30) obtained by regression of experimental data in this research	
		Calculated using experimental f'_m and E_m	Calculated using regression f'_m and E_m values	Calculated using experimental f'_m and E_m	Calculated using regression f'_m and E_m values
NHL5	0.0114	0.0010 {−91}	0.0013 {−88}	0.0020 {−82}	0.0026 −77}
NHL3.5	0.0158	0.0016 {−90}	0.0014 {−91}	0.0030 {−81}	0.0026 {−84}
NHL2	0.0159	0.0027 {−83}	0.0022 {−86}	0.0043 {−73}	0.0039 {−75}
CL90	0.0200	0.0037 {−82}	0.0028 {−86}	0.0510 {−74}	0.0040 {−80}
M6	0.0080	0.0006 {−92}	0.0007 {−91}	0.0017 {−79}	0.0014 {−82}

Table 11
Comparison of masonry compressive strength measured in the laboratory with values calculated using the regression models in Table 1. {} Values represent the percentage error between experimental and model estimated results.

Masonry compressive strength (f'_m) calculated using models in literature and % error between experimental and model estimated results(N/mm^2)									
	Age	f'_m Experimental	Eurocode 6 [22]	Bennett et al. [17]	Dayaratnam [18]	MSJC [19]	Kaushik [10]	GVR) [20]	H & M [21]
NHL5	28 days	4.57	4.46 {−2}	3.83 {−16}	1.93 {−58}	2.78{−39}	3.38 {−26}	3.44 {−25}	1.62 {−64}
	6 months	6.68	6.24 {−7}	3.83 {−43}	3.39 {−49}	2.78 {−58}	4.84 {−43}	4.00 {−43}	2.05 {−69}
NHL3.5	28 days	4.23	4.45 {5}	3.83 {−10}	1.93 {−54}	2.78 {−34}	3.83 {−20}	3.44 {−19}	1.62 {−62}
	6 months	6.43	5.73 {−11}	3.83 {−41}	2.94 {−54}	2.78 {−57}	4.42 {−18}	3.85 {−40}	1.93 {−70}
NHL2	28 days	3.25	3.58 {10}	3.83 {18}	1.34 {−59}	2.78 {−15}	2.68 {−18}	3.13 {−14}	1.40 {−57}
	6 months	4.00	3.97 {−1}	3.83 {−4}	1.59 {−60}	2.78 {−31}	2.99 {−25}	3.27 {−18}	1.50 {−63}
CL90s	28 days	0.74	2.57 {248}	3.83 {417}	0.77 {4}	2.78 {275}	1.88 {154}	2.70 {264}	1.11 {50}
	6 months	3.28	3.28 {0}	3.83 {17}	1.16 {−65}	2.78 {−15}	2.44 {−26}	3.00 {−8}	1.31 {−60}
M6	28 days	5.75	6.13 {7}	3.83 {−34}	3.29 {−43}	2.78 {−52}	4.75 {−17}	3.97 {−31}	2.03 {−34}
	6 months	8.12	7.30 {−10}	3.83 {−53}	4.39 {−46}	2.78 {−66}	5.91 {−27}	4.35 {−46}	2.33 {−71}

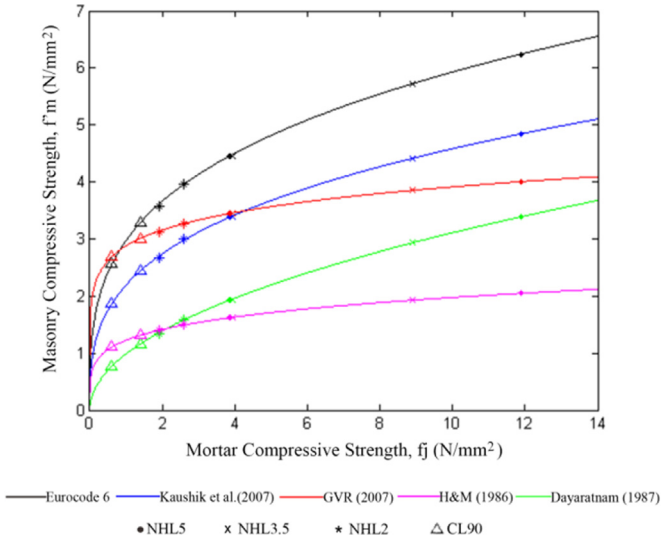

Fig. 6. Models from the literature (Table 1) of masonry compressive strength.

except Eurocode 6, become less accurate predictors over time, and at 6 months, they either significantly overestimate or underestimate the masonry compressive strength.

Stress–strain curves that describe the relationship between applied stress and strain of masonry in compression have been proposed by previous authors [8,10,13,42]. These models were compared with the experimental curves obtained in this research (Fig. 7).

Fig. 7 shows that the experimental results consistently agree with the stress–strain predictions proposed by Kaushik et al. [10]. Therefore, the model proposed by Kaushik *et al.*[10] provides the most accurate estimate of the stress–strain of lime and PC-lime mortar masonry when the peak strain and elastic modulus are experimentally known. However, poor predictions of the stress–strain characteristics were found by other models as they are unable to account for the relatively large deformation associated with lime-mortar masonry. Priestley and Elder [42] as well as Eurocode 6 [8], allow for only limited strains in the rising curve. Furthermore, for Eurocode 6, the descending curve is only applicable to mortars with compressive strength greater than approximately 7 N/mm^2 and hence no downward curvature is seen for lime masonry in Fig. 7. Other models perform well over limited ranges such as the model proposed by Knutson [42] which performs reasonably well but only up to approximately 30% of the ultimate stress (σ_{max}); a divergent characteristic identified in the stress–strain of hollow block masonry bound with flexible cement-lime mortars. If the Knutson model is adjusted (by obtaining the elastic modulus as the tangent modulus (E_0) rather than the linear portion of the stress–strain diagram) and this incorporated in the model, the agreement with experimental curves improves (Fig. 7).

6. Conclusion

The experimental results evidenced that, as the hydraulic grade of the mortar increases, the influence of masonry stiffness (and thus mortar strength and stiffness) on the masonry compressive strength becomes smaller. The influence of masonry stiffness on masonry compressive strength lowers as masonry strength tends towards a maximum. This may be related to the failure mechanisms associated with the lateral tensional capacity of the brick.

The results also evidenced that, as noted by former authors, the properties of the mortar have a strong impact on the deformation of masonry, and that the relationship between stress and strain becomes increasingly non-linear as mortar strength decreases. Stress–strain curves that describe the relationship between applied stress and strain of masonry in compression by former authors were compared with the experimental curves obtained in this research. The experimental results consistently agree with the stress–strain predictions proposed by Kaushik *et al.*[10] however poor predictions of the stress–strain characteristics were found by other models as they are unable to account for the relatively large deformation associated with lime-mortar masonry.

This research has established prediction models to estimate the characteristic compressive strength of lime-mortar masonry using regression analysis of experimental data. Accurate models have been developed for NHL and cement-lime masonry, but the model for hydrated lime bound masonry is less accurate due to the wide disparity between the experimental strengths of the mortar and brick on which the regression is based.

Based on the regression analysis of the experimental data in this research, three relationships between masonry elastic modulus and compressive strength are proposed for PC-lime; hydraulic lime; and feebly hydraulic/hydrated lime masonries respectively. According to the experimental results, the masonry elastic modulus (E_m) reaches values between 82 and 231 times the masonry characteristic compressive strength and their relationship is

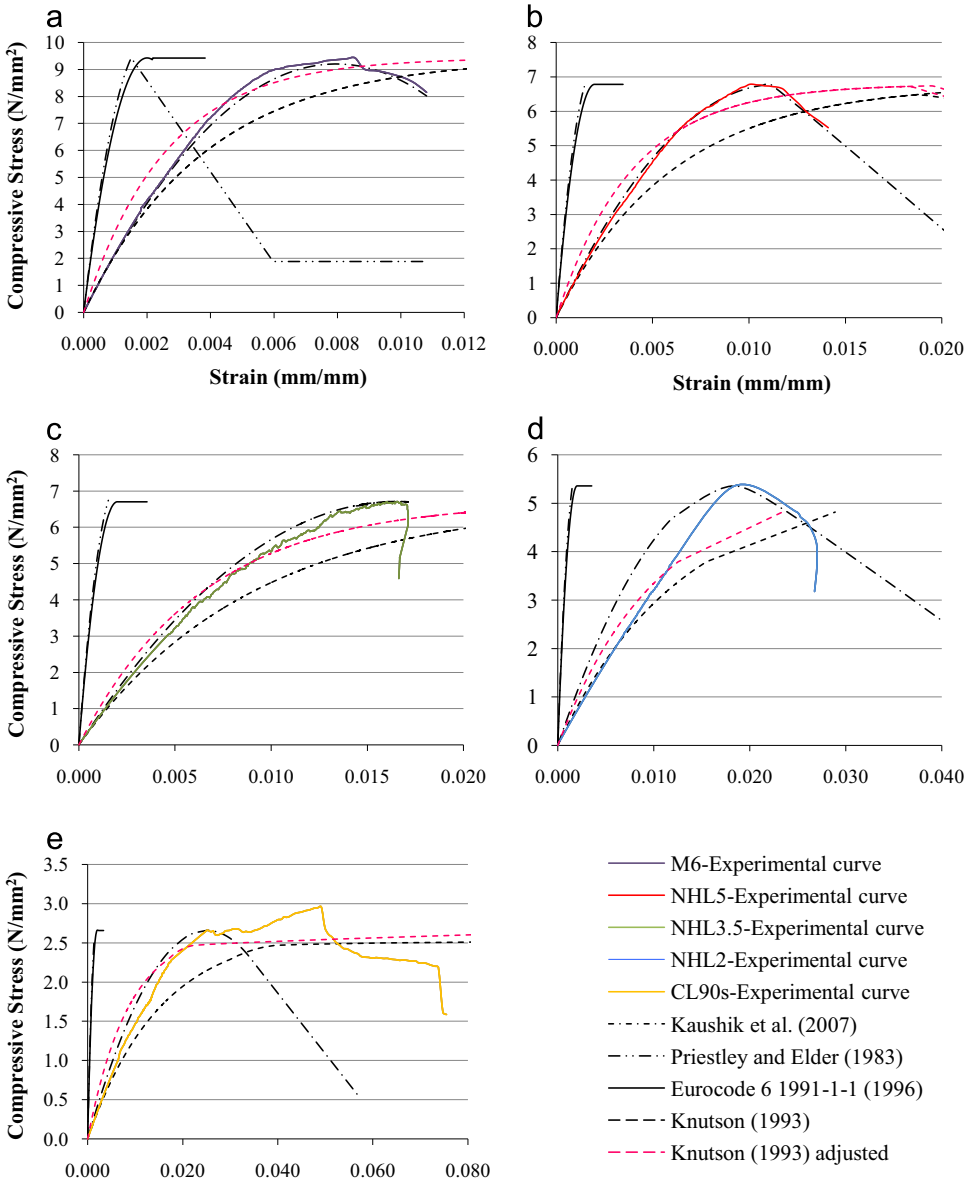

Fig. 7. Comparison of experimental stress–strain characteristics of lime-mortar masonry with models in the literature.

nonlinear. These values are lower than those reported by previous authors for cement bound masonry due to the low stiffness and large deformability of lime mortar masonry. In contrast, the equation deducted by regression did not provide an accurate prediction of masonry peak strain.

Eurocode 6 provided the best predictions for the estimation of the compressive strength of lime and cement-lime masonry based on the strength of their components. It provided an accurate estimation of 28-day characteristic compressive strength of NHL 2, 3.5 and 5 brick-lime masonry. All the existing models vastly overestimate the strength of the hydrated lime mortar (CL90s) masonry at 28 days, however, Eurocode 6 becomes an accurate predictor after 6 months (0–17% error), when the mortar has acquired most of its final strength and stiffness. Except for Eurocode 6, the models significantly underestimate the compressive strength of the hydraulic lime (NHL3.5/5) and cement-lime masonry at all times (an exception is the NHL3.5 masonry at 28 days, whose strength is underestimated, by all models, with a 10% error).

References

[1] A. Zucchini, P.B. Lourenço, Mechanics of masonry in compression: Results from a homogenisation approach, Comput. Struct. 85 (3–4) (2007) 193–204.
[2] A.W. Hendry, Structural Masonry, Macmillan Education, Limited, 1998.
[3] H.K. Hilsdorf, Investigation into the failure mechanism of brick masonry loaded in axial compression, In: Designing, Engineering and Constructing with Masonry Products, Gulf Publishing Company, 1969, pp. 34–41.
[4] W. McNary, D. Abrams, Mechanics of masonry in compression, J. Struct. Eng. 111 (4) (1985) 857–870.
[5] A.T. Vermelfoort, Brick–mortar interaction in masonry under pressure (Ph.D. thesis), Eindhoven University of Technology, The Netherlands, 2005.
[6] L. Binda, A. Fontana, G. Frigerio, Mechanical behaviour of brick masonries derived from unit and mortar characteristics, In: Proceedings of 8th International Brick and Block Masonry Conference, Dublin, Ireland, 1988.
[7] L. Binda, C. Tiraboschi, S. Abbaneo, Experimental research to characterise masonry materials, Mason. Int. 10 (3) (1997) 92–101.
[8] EN 1996-1 and 2: 2005, Eurocode 6-Design of masonry structures. Part 1-1: - General rules for buildings—reinforced and unreinforced masonry, Design of masonry structures. Design Considerations, Selection of Materials and Execution of Masonry. European Committee for Standardisation CEN, Brussels, 2006.
[9] EN 771–1:2003 – Specification for masonry units, Part 1: Clay masonry units, European Committee for Standardisation CEN, Brussels, 2003.
[10] H.B. Kaushik, D.C. Rai, S.K. Jain, Stress-strain characteristics of clay brick masonry under uniaxial compression, J. Mater. Civ. Eng 19 (9) (2007) 728–739.

[11] D. García, J.T. San-José, L. Garmendia, R. San-Mateos, Experimental study of traditional stone masonry under compressive load and comparison of results with design codes, Mater. Struct. 45 (7) (2012) 995–1006.
[12] C.T. Grimm, Strength and related properties of brick masonry, J. Struct. Div 101 (1) (1975) 217–232.
[13] M.J.N. Priestley, D.M. Elder, Stress–strain curves for unconfined and confined concrete masonry, ACI J. Proc. 80 (3) (1983) 728–739.
[14] R.H. Atkinson, J.L. Nolan, A proposed failure theory for brick masonry in compression, In: Proceedings of the 3rd Canadian Masonry Symposium, 1983, pp. 510–517.
[15] T. Paulay, M.J.N. Priestley, Seismic Design of Reinforced Concrete and Masonry Buildings, 1 edition, Wiley-Interscience, New York, 1992.
[16] B. Ewing, M. Kowalsky, Compressive behavior of unconfined and confined clay brick masonry, J. Struct. Eng. 130 (4) (2004) 650–661.
[17] R. Bennett, K. Boyd, R. Flanagan, Compressive properties of structural clay tile prisms, J. Struct. Eng 123 (7) (1997) 920–926.
[18] P. Dayaratnam, Brick and Reinforced Brick Structures, Oxford & IBH, 1987.
[19] MSJC, MSJC, Masonry Standards Joint Committee, Building code requirements for masonry structures," ACI 530-02/ASCE 5-02/TMS 402-02, American Concrete Institute, Structural Engineering Institute of the American Society of Civil Engineers, The Masonry Society, Detroit, 2002.
[20] K.S. Gumaste, K.S.N. Rao, B.V.V. Reddy, K.S. Jagadish, Strength and elasticity of brick masonry prisms and wallettes under compression, Mater. Struct. 40 (2) (2007) 241–253.
[21] A.W. Hendry, M. Malek, Characteristic compressive strength of brickwork from collected test results, Mason. Int. 7 (1986) 15–24.
[22] International Masonry Society, Eurocode for masonry, EN 1996-1-1 and EN 1996-2: Guidance and Worked Examples, International Masonry Society, Stoke-on-Trent, 2009.
[23] R.G. Drysdale, M. Khattab, In-plane behavior of grouted concrete masonry under biaxial tension–compression, ACI Struct. J. 92 (6) (1995) 653–664.
[24] A.T. Vermelfoort, Strength-size relationships for Aircrete under compression, In: Autoclave Aerated Concrete. Innovation and Development, Taylor & Francis, 2005, pp. 357–364.
[25] G. Mohamad, P.B. Lourenço, H.R. Roman, Mechanics of hollow concrete block masonry prisms under compression: review and prospects, Cem. Concr. Compos. 29 (3) (2007) 181–192.
[26] BS EN 459-1:2010 – Building lime, Definitions, specifications and conformity criteria. European Committee for Standardisation CEN, Brussel, 2010.
[27] R. Hanley, S. Pavía, A study of the workability of natural hydraulic lime mortars and its influence on strength, Mater. Struct. 41 (2) (2008) 373–381.
[28] S. Pavía, R. Hanley, Flexural bond strength of natural hydraulic lime mortar and clay brick, Mater. Struct. 43 (7) (2010) 913–922.
[29] EN 459-2:2010 – Building lime. Part 2: Test Methods, European Committee for Standardisation CEN, Brussels, 2010.
[30] EN 196-1:2005 – Methods of testing cement. Determination of strength. European Committee for Standardisation CEN, Brussels, 2005.
[31] EN 1052–1:1999 – Method of test masonry, Part 1: Determination of Compressive Strength, European Committee for Standardisation CEN, Brussels, 1999.
[32] EN 772-1:2011, Methods of test for masonry units. Determination of compressive strength, European Committee for Standardisation CEN, Brussels, 2011.
[33] EN 12372:2006 – Determination of flexural strength under concentrated load, European Committee for Standardisation CEN, Brussels, 2006.
[34] EN 1936:2006 – Natural stone test methods, Determination of REAL DENsity and Apparent Density, and of Total and Open Porosity, European Committee for Standardisation CEN, Brussels, 2006.
[35] EN 772-11:2011, Methods of Test for Masonry Units, Determination of Water Absorption of Aggregate Concrete, Autoclaved Aerated Concrete, Manufactured Stone and Natural Stone Masonry Units due to Capillary Action and the Initial Rate of Water Absorption of Clay Masonry Units, European Committee for Standardisation CEN, Brussels, 2011.
[36] A. Costigan, S. Pavía, Influence of the mechanical properties of lime mortar on the strength of brick masonry, In: J. Valek et al. (Eds.), Historic Mortars: Characterization, Assessment and Repair, RILEM Book series 7, RILEM, 2012, pp. 359–372, http://dx.doi.org/10.1007/978-94-007-4635-0_1.
[37] A. Costigan, S. Pavía, Influence of the hydraulic strength of mortar on the mechanical behaviour of lime mortar masonry, in: HMC 2010, Prague, ed. by Institute of Theoretical and Applied Mechanics, RILEM, 2010.
[38] A. Costigan, S. Pavía, Mechanical properties of clay brick masonry bound with hydraulic limes and hydrated calcium lime, In: W. Jäger, B. Haseltine, A. Fried (Eds.), Proceedings of the 8th International Masonry Conference, Dresden, July 2010, pp. 903–914.
[39] A.J. Francis, C.B. Horman, L.E. Jerrems, The effect of joint thickness and other factors on compressive strength of brickwork In: Proceedings of 2nd International Brick Masonry Conference, Stoke-on-Trent, pp. 31–37.
[40] A.C.I. and S.E.I.T.M. Society, ACI 530-08 Building Code Requirements and Specification for Masonry Structures, F First Edition edition, Boulder, Colo.; Farmington Hills, MI; Reston, Amer Society of Civil Engineers, VA, 2008.
[41] G. Mohamad, P.B. Lourenço, H.R. Roman, Mechanical behavior assessment of concrete block masonry prisms under compression, In: Proceedings of International Conference on Concrete for Structures, 2005, pp. 261–268.
[42] H.H. Knutson, The stress–strain relationship for masonry, Mason. Int. 7 (1) (1993) 31–33.